THE JOURNAL OF BIOLOGICAL CHEMISTRY
Vol. 277, No. 1, Issue of January 4, pp. 23–31, 2002
Printed in U.S.A.

Role of Interfacial Hydrophobic Residues in the Stabilization of the Leucine Zipper Structures of the Transcription Factors c-Fos and c-Jun*

Received for publication, May 18, 2001, and in revised form, September 21, 2001
Published, JBC Papers in Press, October 15, 2001, DOI 10.1074/jbc.M104556200

Reinhard I. Boysen‡, Agnes J. O. Jong‡, Jackie A. Wilce§, Glenn F. King¶, and Milton T. W. Hearn‡‖

From the ‡Centre for Bioprocess Technology, Department of Biochemistry and Molecular Biology, Monash University, P. O. Box 13D, Victoria 3800, the §Department of Chemistry and Biochemistry, University of Western Australia, Nedlands, West Australia 6907, Australia, and the ¶Department of Biochemistry, University of Connecticut Health Center, Farmington, Connecticut 06032

This study documents a new and versatile experimental approach to study the relative stabilization energetics of recombinant polypeptide and protein mutants. In particular, the effect of temperature change over the range of T = 278–338 K on the thermodynamics of interaction of several leucine zipper coiled-coil polypeptides related to the transcription factors, c-Fos and c-Jun, following binding to immobilized *n*-octyl ligands has been determined. Plots of the change in heat capacity, ΔC_p^0, *versus* T, in combination with the corresponding van't Hoff plots, allow the energetics of the interaction of polypeptides with *n*-octyl ligands to be rationalized and the respective mid-point transition temperatures, T_m values, determined for the melting of their supramolecular structures. The derived experimental data correlated well with information available from other procedures, confirming that this new approach provides complementary insight into the interaction thermodynamics and the molecular nature of the thermal stability of recombinant polypeptides in non-polar or other types of chemical environments.

Fos and Jun belong to a family of eukaryotic transcription factors (1, 2) that heterodimerize to form complexes capable of binding to 5′-TGAGTCA-3′ DNA. Besides the DNA-binding domain, Fos and Jun contain a leucine zipper motif, consisting of a heptad repeat, denoted $(abcdefg)_n$, with hydrophobic residues at positions *a* and *d* involved in the dimer interface with five Leu residues spaced periodically along the polypeptide chain at every seventh position (3, 4). This heptad repeat motif has received considerable attention over the past decade because of its fundamental role in determining the activity of eukaryotic transcription factors. The binding orientation of the Fos/Jun heterodimer to palindromic AP-1 regulator elements is believed to be controlled by indirect recognition of differences in DNA structure between flanking sequences on opposite sides of the AP-1 site (5), coupled with minimization of the electrostatic free energy of the Fos-Jun-AP-1 complex through long range electrostatic interactions within the nucleoprotein complex (6). Both NMR spectroscopic (7, 8) and x-ray diffraction (9, 10) studies have shown that the leucine zipper is formed from two parallel coiled-coil α-helices, which wrap around each other with a slightly left-handed super-helical twist. The presence of Leu at position *d* is highly conserved among leucine zippers (11). Other amino acid residues, such as Glu and Lys, at positions *e* and *g* are capable of forming inter-helical salt bridges, whereas residues at position *b*, *c,* and *f* are distal to the dimer interface and solvent-exposed (12, 13).

The hydrophobic effect provides one of the primary forces in the formation of coiled-coil polypeptides. Electrostatic interactions between solvent-exposed surface regions of the polypeptide are usually weak and contribute little to stability (14). Inter-helical salt bridges, as found in Fos/Jun heterodimers, can contribute to the coiled-coil stability (9, 10). However, this structural contribution depends on the hydrophobicity of the amino acid residues in the microenvironment of these charge interactions. Partially non-aqueous solvent conditions favor salt bridge formation with leucine zippers, with salt bridges tending to reduce further the solvent accessibility of the hydrophobic core. The *e* and *g* positions of the Fos leucine zipper mainly contain negatively charged residues, whereas at these positions the Jun leucine zipper contains positively charged residues. Because the Fos/Jun heterodimer exhibits higher stability compared with the Fos/Fos or Jun/Jun homodimers, electrostatic attractions have been proposed (9, 15) as the primary driving force for the *in vivo* heterodimerization of these polypeptides. However, recent NMR studies (7, 8) have shown that at acidic pH values intermolecular electrostatic interactions in the homodimer are largely ablated; yet stable dimers still form. Furthermore, at acidic pH values the T_m value for the Fos/Jun heterodimer actually increases (15).

In this investigation, the stability in non-polar environments of several recombinant polypeptides, corresponding to the leucine zipper regions of human c-Fos (residues Leu^{161}–Ala^{199}) and c-Jun (residues Arg^{276}–Asn^{314}), has been investigated, allowing the role of interfacial hydrophobic residues in the stabilization of leucine zipper structures to be studied further. With these r[1]-Fos and r-Jun leucine zipper (LZ) mutant polypeptides, a two Gly residue insert (to allow for greater flexibility) and a Cys residue (to permit disulfide bond formation) were introduced at the N terminus to enable the extent of monomer/dimer formation in different solvent systems to be

* This work was supported by the Australian Research Council and the National Health and Medical Research Council of Australia. The costs of publication of this article were defrayed in part by the payment of page charges. This article must therefore be hereby marked "*advertisement*" in accordance with 18 U.S.C. Section 1734 solely to indicate this fact.

‖ To whom correspondence should be addressed. Tel.: 61 3 99 05 37 20; Fax: 61 3 9905 5882; E-mail: milton.hearn@med.monash.edu.au.

[1] The abbreviations used are: r, recombinant; ACN, acetonitrile; DTT, dithiothreitol; EEC, entropy-enthalpy compensation; ESI-MS, electrospray ionization-mass spectrometry; LZ, leucine zipper; RP-HPLC, reversed-phase high-performance liquid chromatography.

controlled. For example, the r-JunLZ dimer is known (7) to adopt a symmetrical coiled-coil structure of parallel α-helices in aqueous solutions. These structures are expected to be stabilized further by the presence of low to intermediate concentrations of acetonitrile (16–18). The introduction of the additional non-native $(Gly)_2$-Cys residues at the N terminus of these recombinant mutants is unlikely to affect α-helix formation but was expected to permit stabilization of the coiled-coil structure. Leucine zipper homodimers containing either small or large hydrophobic residues in positions *a* or *d* can produce packing defects at the interface of the two helices, and this can potentially destabilize the coiled-coil structure. If complementary positions on both helices have small hydrophobic residues, these residues cannot interact with each other and result in an increased solvent-accessible region at the hydrophobic interface. Analysis of the tertiary structure of the r-JunLZ homodimer has shown (8) that a cavity forms at the dimer interface because of the parallel arrangement of the side chains of the two associating Ala^{298} residues, resulting from their orientation away from the dimer interface. It has also been found (19) that substitution of the Ala^{298} residue by Val in the hydrophobic core of the Jun leucine zipper polypeptide can reduce this "packing defect" and thus can significantly affect the oligomerization state of the polypeptide. Mutants in which Ala^{298} is replaced with a bigger hydrophobic residue, *e.g.* Val, Ile, or Leu, consequently have higher stability as shown by their thermal melt profiles in CD spectroscopy (20). It has also been suggested that the packing defect evident with the Ala^{298}–Jun/Jun homodimer has the biological function to allow fast strand exchange *in vivo* and to allow the basic domain leucine zipper dimerization to be under kinetic rather than thermodynamic control (8, 21). For these reasons, the mutant Jun($Ala^{298} \rightarrow$ Ile) was investigated in the present study as a monomer as well as a homodimer. Because of the known influence of acetonitrile on the stability of α-helical and coiled-coil polypeptides (22–24), low pH acetonitrile/water mixtures with volume fractions of acetonitrile in the range of 0.28–0.41, corresponding to a concentration range of 6.8-10.0 M, were selected for these experiments. A recently developed thermometric approach (25–27) was then used to evaluate the temperature-dependent uncoiling behavior of these recombinant Fos and Jun leucine zipper polypeptides in the presence of hydrophobic *n*-octyl ligands and, in particular, to quantify the impact of a single amino acid residue substitution (at the heptad position *a* from Ala $\rightarrow$ Ile) in the hydrophobic interface on dimer stability of the Jun leucine zipper.

EXPERIMENTAL PROCEDURES

Apparatus—All thermometric measurements were performed on a Agilent HP1090 instrument and HP Chemstation (Agilent, Waldbronn, Germany) with polypeptide detection at 215 nm.

Chemicals and Reagents—Acetonitrile (HPLC grade) was obtained from Biolab Scientific Pty. Ltd. (Sydney, Australia) and trifluoroacetic acid from Auspep Pty. Ltd. (Melbourne, Australia). Water was distilled and deionized in a Milli-Q system (Millipore, Bedford, MA). Recombinant polypeptides corresponding to the LZ domain of human c-Jun (Arg^{276}–Asn^{314}; r-JunLZ), c-Fos (residues Leu^{161}–Ala^{199}; r-FosLZ), and the r-JunLZ mutant containing the single amino acid substitution $Ala^{298} \rightarrow$ Ile, r-JunA298I LZ, were prepared and purified as described previously (19, 20). The leucine zipper domains contained an additional N-terminal hexapeptide GSMCGG and a non-native C-terminal Tyr residue, whereby the CGG linker facilitated disulfide bond formation of the dimers[2] and the Tyr residue facilitated UV detection at 280 nm during purification of the recombinant polypeptides.

Control of Dimerization—Monomers or dimers of r-FosLZ and r-JunLZ were prepared by incubating the polypeptide at a final concentration of 0.5 mg/ml in either (i) 30% ACN, 0.09% trifluoroacetic acid, 69.91% water (v/v/v); (ii) the monomerization buffer (0.2 M DTT, 0.1 M Tris-HCl, pH 8.3); or (iii) the dimerization buffer (1 mM EDTA, 0.1 M Tris-HCl, pH 8.3 (19)) for at least 1 h at ambient temperatures. An aliquot of 30 μl of the incubates was taken, and the polypeptides were analyzed using a Waters 600/486 analytical HPLC system with TSK-ODS-120 T columns (150 $\times$ 4.6 mm inner diameter, Tosoh Corp., Yamaguchi, Japan), packed with 5 μm of octadecyl-silica. The eluents employed were as follows: eluent A, 0.1% (v/v) trifluoroacetic acid in water; eluent B, 0.09% (v/v) trifluoroacetic acid in 60% (v/v) acetonitrile/water, with a linear gradient of 0–100% B over 60 min. UV detection at 214 nm and a flow rate of 1 ml/min were used. The major peak was collected and analyzed for the monomer/dimer state by ESI-MS.

Electrospray Ionization Mass Spectrometry (ESI-MS)—Electrospray mass spectra were generated by using a Micromass platform (II) quadrupole MS with electrospray source and Masslynx NT version 3.2 software (Micromass, Cheshire, UK). The r-FosLZ and r-JunLZ polypeptides in 1:1 (v/v) ACN/water with 3% (v/v) formic acid were infused into the instrument at a speed of 10 μl per min. The ESI-MS data for the r-Fos/r-Jun polypeptides were acquired at 70 °C at 55/50 V for the monomers and at 70/60 V for the dimers, respectively. The spectra were obtained from mass/charge (*m/z*) range of 200–2000.

Calculation of Accessible Surface Area—The accessible surface area for the $Jun^{272–315}$ leucine zipper domain from *Homo sapiens* (8) was calculated using the programs SCRIPT1 and SCRIPT2 at www.bork.embl-heidelberg.de/ASC/asc2.html (28, 29). The Protein Data Bank file identifier (code 1JUN) was taken from the Protein Data Bank at www.rcsb.org/pdb/ (30, 31).

Determination of the k′ Values for the r-FosLZ and r-JunLZ Polypeptide Mutants—Bulk solvents were filtered and degassed by sparging with helium. The k' (where k' is $K_a \times V_S/V_M = K_a \times \Phi = e^{(-\Delta G_a^0/RT)} \times \Phi$) measurements (32) were performed using different solvent combinations of fixed composition containing 0.09% (v/v) trifluoroacetic acid and acetonitrile contents between 28 and 41% (v/v) in 1% increments in water, with Zorbax 300SB-C8 columns, 150 $\times$ 4.6 mm inner diameter (Agilent Inc., Littlefalls, DE) operated at a flow rate of 1 ml/min and at temperatures between 278 and 338 K in 5 K increments. Temperature was controlled by immersing these columns in a thermostated column coolant jacket coupled to a recirculating cooler (Colora Messtechnik GmbH, Lorchwutt, Germany). Solutions of the polypeptides were prepared at a concentration between 0.5 and 1 mg/ml in 0.09% (v/v) trifluoroacetic acid/water. The sample size varied between 2–25 μg, depending on the k' value. All data points were derived from at least duplicate measurements. The relative standard deviations of the replicates for the k' measurements were $\leq \pm 1\%$. Similarly, the precision in the temperature measurements was the $\leq \pm 0.5$ K over the studied temperature range. The total volume, V_T, the stationary phase volume, V_S, the free solvent phase volume, V_M, and the phase ratio, Φ, of the system at constant pressure were determined (32, 33) using the non-interactive solute, sodium nitrate. Metacresol was employed as a low molecular weight standard to ensure that reproducibility and stability of the two-phase system occurred over the complete range of temperatures investigated throughout the duration of the experiments.

Thermodynamic Considerations—According to Nernst's law, for a reversible, equilibrium interaction between a polypeptide/protein and an immobilized ligand(s) supported on an inert matrix, the relationship between the equilibrium association constant, K_a, and the mass of the polypeptide in the bound (m_S) and free (m_M) states can be expressed as shown in Equation 1,

$$K_a = \frac{m_S\, V_M}{m_M\, V_S} \qquad \text{(Eq. 1)}$$

where V_S and V_M are the volume of the immobilized ligand/support material and the volume of the bulk solution, respectively. For a two-phase system, the ratio V_S/V_M can be represented as the phase ratio, Φ, whereas the ratio m_S/m_M for a calibrated system of known V_S and V_M values corresponds to the unitless parameter, k' (25–27). When measured with solid/liquid two-phase systems at equilibrium, k' can also be expressed in terms of K_a, and thus k' can be related to the Gibbs free energy change (due to association of the polypeptide P_i with the immobilized non-polar ligands), ΔG_a^0, for a polypeptide-ligand interaction as shown in Equation 2,

$$k' = K_a \times \frac{V_S}{V_M} = K_a \times \Phi = e^{(-\Delta\, G_a^0/RT)} \times \Phi \qquad \text{(Eq. 2)}$$

[2] The nomenclature used in this paper for the r-FosLZ and r-JunLZ leucine zipper homo- and heterodimers follows previous literature on disulfide-linked coiled coils where two monomeric coils dimerize to form the stabilized coiled coil and can be contrasted to higher order oligomer formation.

where R is the universal gas constant, and T is the absolute temperature in degrees Kelvin. Similarly, the dependence of the k' of a polypeptide in association with a non-polar n-alkyl ligand(s) on the temperature, T, for a system of defined phase ratios at constant pressure and solvent composition can be described (25–27, 32–34) in terms of the Gibbs-Helmholtz relationship, *e.g.* the thermodynamic basis of the interaction can be evaluated from the expression shown in Equation 3,

$$\ln k' = \frac{-\Delta H_a^0}{RT} + \frac{\Delta S_a^0}{R} + \ln\Phi \qquad \text{(Eq. 3)}$$

where ΔH_a^0 and ΔS_a^0 are the apparent changes in enthalpy and entropy of interaction due to the association of the polypeptide P_i with the immobilized non-polar ligands. At equilibrium, $\ln K_e$ and $\ln k'$ (where $\ln k'$ is the logarithm of the unitless factor, k') bear the same formal relationship to the variation in the standard free energy, ΔG_a^0, for these reversible polypeptide-non-polar ligand interactions. The contribution of the corresponding changes in enthalpy, ΔH_a^0, and entropy, ΔS_a^0, to ΔG_a^0 can moreover be quantitatively evaluated from Equation 4,

$$\Delta G_a^0 = \Delta H_a^0 - T\Delta S_a^0 \qquad \text{(Eq. 4)}$$

Isothermic processes are expected for rigid organic molecules, amino acids, or small peptides, which have no well developed secondary structure and little or no possibility to change their hydrophobic contact areas in association with non-polar ligands at different temperatures. If the interaction of a polypeptide with the non-polar ligand(s) also involves a simple isothermic process, linear van't Hoff plots, *i.e.* linear plots of *lnk' versus* 1/T, are anticipated, with the change in heat capacity for the interaction $\Delta C_p^0 = 0$, and independent of T (25, 27, 32). On the other hand, for polypeptides and proteins that undergo conformational or self-association processes at high (or low) temperatures under specified conditions, homothermic or heterothermic processes (25) are expected. When the latter processes occur between a polypeptide or protein and immobilized n-alkyl ligands, the dependence of $\ln k'$ on T can be approximated (25, 27, 32) by the polynomial expression shown in Equation 5,

$$\ln k' = b_{(0)} + \frac{b_{(1)}}{T} + \frac{b_{(2)}}{T^2} + \frac{b_{(3)}}{T^3} + \ldots\ldots\ldots + \ln\Phi \qquad \text{(Eq. 5)}$$

where the coefficients for polynomial dependency of $\ln k'$ on 1/T, $b_{(0)}$, $b_{(1)}$, $b_{(2)}$, $b_{(3)}$ . . . , represent molecular descriptor parameters for the polypeptide or protein and can be evaluated from the lnk' *versus* 1/T plots using non-linear regression procedures. With highly stabilized polypeptides or globular proteins, such as cytochrome *c*, their binding behavior with immobilized non-polar ligands typically follows parabolic van't Hoff dependences (35–38) with their interaction thermodynamics successfully interpreted in terms of the quadratic relationship shown in Equation 6,

$$\ln k' = b_{(0)} + \frac{b_{(1)}}{T} + \frac{b_{(2)}}{T^2} + \ln\Phi \qquad \text{(Eq. 6)}$$

with the change in enthalpy of association given by Equation 7,

$$\Delta H_a^0 = -R\left[b_{(1)} + \frac{2b_{(2)}}{T}\right] \qquad \text{(Eq. 7)}$$

whereas the change in entropy of association and change in heat capacity of association can be evaluated from Equations 8 and 9,

$$\Delta S_a^0 = R\left[b_{(0)} - \frac{b_{(2)}}{T^2}\right] \qquad \text{(Eq. 8)}$$

$$\Delta C_p^0 = R\left[\frac{2b_{(2)}}{T^2}\right] \qquad \text{(Eq. 9)}$$

For polypeptide-non-polar ligand interactions that follow more complex heterothermic processes, where $\Delta C_p^0 \neq 0$ and a non-linear function of T, sigmoidal van't Hoff plots have been predicted (25–27) with the dependences of $\ln k'$ on 1/T and the corresponding dependences of ΔH_a^0, ΔS_a^0, and ΔC_p^0 on T following the relationships shown in Equations 10–13.

$$\ln k' = b_{(0)} + \frac{b_{(1)}}{T} + \frac{b_{(2)}}{T^2} + \frac{b_{(3)}}{T^3} + \frac{b_{(4)}}{T^4} + \ln\Phi \qquad \text{(Eq. 10)}$$

$$\Delta H_a^0 = -R\left[b_{(1)} + \frac{2b_{(2)}}{T} + \frac{3b_{(3)}}{T^2} + \frac{4b_{(4)}}{T^3}\right] \qquad \text{(Eq. 11)}$$

$$\Delta S_a^0 = R\left[b_{(0)} - \frac{b_{(2)}}{T^2} - \frac{2b_{(3)}}{T^3} - \frac{3b_{(4)}}{T^4}\right] \qquad \text{(Eq. 12)}$$

$$\Delta C_p^0 = R\left[\frac{2b_{(2)}}{T^2} + \frac{6b_{(3)}}{T^3} + \frac{12b_{(4)}}{T^4}\right] \qquad \text{(Eq. 13)}$$

Inflection points will be evident in these non-linear van't Hoff plots, representing the midpoint melting temperatures, T_m values, for the transition between the folded/unfolded state or in the case of coiled-coil polypeptides the transition between the dimer and monomer states. Under conditions of homo- or heterothermal binding, *e.g.* processes described by Equations 10–13, the T_m for a folded polypeptide in the presence of a non-polar ligand(s) can be calculated[3] from Equation 14,

$$\frac{1}{T_m} = -\frac{b_{(3)}}{4b_{(4)}} \pm \frac{\sqrt{\left(\frac{b_{(3)}}{2b_{(4)}}\right)^2 - \left(\frac{4b_{(2)}}{6b_{(4)}}\right)}}{2} \qquad \text{(Eq. 14)}$$

Similarly, the temperatures at which the values of ΔH_a^0 and ΔS_a^0 become 0 for a particular polypeptide/protein under a specified set of conditions can be defined as the compensation temperatures, $T_{H(\varphi=i)}$ and $T_{S(\varphi=i)}$, respectively, which can be calculated[3] from Equations 15 and 16,

$$T_{H(\varphi=i)} = \frac{2Rb_{(2)}}{\Delta H_a^0 - Rb_{(1)}} \quad for \quad \Delta H_a^0 = 0 \qquad \text{(Eq. 15)}$$

$$T_{S(\varphi=i)} = \sqrt{\frac{-Rb_{(2)}}{\Delta S_a^0 - Rb_{(0)}}} \quad for \quad \Delta S_a^0 = 0 \qquad \text{(Eq. 16)}$$

The various thermodynamic and extrathermodynamic parameters for the Fos and Jun leucine zipper polypeptides were calculated as a function of T and solvent composition from the experimental data using the *Hephaestus/Eudoxos* software developed in this laboratory, coupled to the Excel version 5.0 program (Microsoft), whereas the statistical analysis involved the Sigma plot 4.01 (Jandel Scientific) linear and non-linear regression analysis. The *Hephaestus/Eudoxos* software is commercially available by contacting Prof. M. T. W. Hearn, Director, Center for Bioprocess Technology, Monash University, Clayton, Victoria 3800, Australia.

RESULTS AND DISCUSSION

Control of Monomer/Dimer Formation—In the current study, the role of interfacial hydrophobic residues in the stabilization of the Jun/Jun homodimer and Fos/Jun heterodimer was chosen for investigation using a new thermometric methodology that permits the interaction thermodynamics of such coiled-coil polypeptide structures to be evaluated. Changes in the secondary structure or dimer assembly of the Fos and Jun leucine zipper polypeptides will alter the hydrophobic contact area of these polypeptides, and this behavior was expected to be reflected in the lnk' *versus* 1/T plots. Prior to undertaking the thermodynamic analyses of the polypeptide-ligand interactions, r-FosLZ and r-JunA298ILZ (Tables I and II) were incubated in different solvent compositions to examine the effect of these conditions on the monomeric or dimeric states of these polypeptides. The incubated samples were then chromatographed under analytical gradient elution RP-HPLC conditions with fractions collected and immediately subjected to ESI-MS (Table III). Monomeric species were obtained for r-FosLZ and r-JunA298ILZ incubated in the presence of DTT as shown in Fig. 1, *A* and *C,* respectively, whereas dimeric species were obtained (Fig. 1, *B* and *D*) for r-FosLZ and r-JunA298ILZ when incubated in a EDTA buffer and 30% (v/v) acetonitrile/water. For these leucine zipper polypeptides, the monomeric species eluted later than the dimeric species from the *n*-octylsilica sorbent, with characteristic retention time shifts toward shorter values following dimerization. For r-FosLZ and r-JunA298ILZ, the decrease in retention time on dimerization was 1.6 and 9.1 min, respectively, under the experimental conditions employed (see "Experimental Procedures"). For both r-FosLZ and r-JunA298ILZ, the retention times were essentially unchanged after incubation in either the dimerization buffer (1 mM EDTA, 0.1 M Tris-HCl, pH 8.3) or 30% (v/v)

[3] R. I. Boysen and M. T. W. Hearn, unpublished results.

TABLE I

Amino acid sequence of engineered Jun leucine zipper domain residues 270–315 from H. sapiens with inserts at positions 270–275 and 315

The natural amino acid sequence is depicted in normal font.

						Helical position[a]						
						g	a	b	c	d	e	f	g
Gly	**Ser**	**Met**	**Cys**	**Gly**	**Gly**	Arg	Ile	Ala	Arg	Leu	Glu	Glu	Lys^{283}
							Val	Lys	Thr	Leu	Lys	Ala	Gln^{290}
							Asn	Ser	Glu	Leu	Ala	Ser	Thr^{297}
							Ala	Asn	Met	Leu	Arg	Glu	Gln^{304}
							Val	Ala	Gln	Leu	Lys	Gln	Lys^{311}
							Val	Met	Asn	**Tyr**^{315}			

[a] The letters a–g refer to the amino acid residue position in the helix according to Ref. 3. The location of the Gly^{270}–Gly^{275} and Tyr^{315} residues are shown in bold with underlines. The location of the Ala^{278} → Ile^{278} substitution is shown as bold with double underline.

TABLE II

Amino acid sequence of engineered Fos leucine zipper domain residues 155–200 from H. sapiens with the location of the Gly^{155}–Gly^{160} and Tyr^{200} residues are shown in bold, underlined

The natural amino acid sequence is depicted in normal font.

						Helical position[a]						
						g	a	b	c	d	e	f	g
Gly	**Ser**	**Met**	**Cys**	**Gly**	**Gly**	Leu	Thr	Asp	Thr	Leu	Gln	Ala	Glu^{168}
							Thr	Asp	Gln	Leu	Glu	Asp	Gln^{175}
							Lys	Ser	Ala	Leu	Gln	Thr	Glu^{182}
							Ile	Ala	Asn	Leu	Leu	Lys	Glu^{189}
							Lys	Glu	Lys	Leu	Glu	Phe	Ile^{196}
							Leu	Ala	Ala	**Tyr**^{200}			

[a] The letters a–g refer to the amino acid residue position the position in the helix according to Ref. 3.

TABLE III

Molecular weights of r-FosLZ (residues 155–200 as in Table II) and r-JunLZ (residues 270–315 as in Table I, except residue 298 which is an Ile) determined with ESI-MS after RP-HPLC purification

The calculated molecular weights correspond to the mono-isotopic values.

Polypeptide	Observed M_r	Calculated M_r	ΔM_r
r-FosLZ monomer	5058.59 ± 0.18	5058.72	0.13
r-FosLZ homodimer	10115.59 ± 0.76	10115.42	−0.17
r-JunLZ A298I monomer	5166.18 ± 1.19	5167.09	0.91
r-JunLZ A298I homodimer	10329.57 ± 3.28	10332.17	2.60

acetonitrile, 0.09% (v/v) trifluoroacetic acid/water, indicting that the latter solvent conditions did not perturb the monomer/dimer equilibrium.

Van't Hoff Measurements—As evident from Fig. 2, *A–D*, the van't Hoff plots for the r-JunLZ dimer, r-JunA298ILZ dimer, r-FosLZ dimer and r-JunA298ILZ monomer were non-linear with differences evident between the dimeric and monomeric forms of these polypeptides. The experimental data were fitted to the expanded form of Equation 4 to ensure that minimal statistical residuals were obtained following least square regression analyses of these data and the derived corresponding values of ΔH_a^0, ΔS_a^0, and ΔC_p^0. The lnk' *versus* 1/T data for the r-JunA298ILZ monomer (Fig. 2*D*) fitted to a second order (dome-shaped) dependence (*cf.* Equations 5–8), whereas the lnk' *versus* 1/T data for the Fos and Jun dimers (Fig. 2, *A–C*) fitted to a fourth order (sigmoidal) dependence, predicted for polypeptides undergoing conformational reorganization and/or subunit dissociation (23, 25). In all cases, correlation coefficient values of $r^2 > 0.9908$ were obtained. Similar dome-shaped (or inverted dome-shaped) dependences between the lnK_e as a function of T have been widely noted for the unfolding of globular proteins and for protein-ligand interactions, including the unfolding of phage T4 lysozyme (39) and the stabilization of the complex between the *lac* repressor and the O^{sym} operator (40).

The occurrence of dome-shaped or sigmoidal van't Hoff plots for these leucine zipper polypeptides is consistent with the standard free energy of association, ΔG_a^0, of the polypeptide-non-polar ligand complex reaching a maximum value at a specific temperature. The standard free energy changes associated

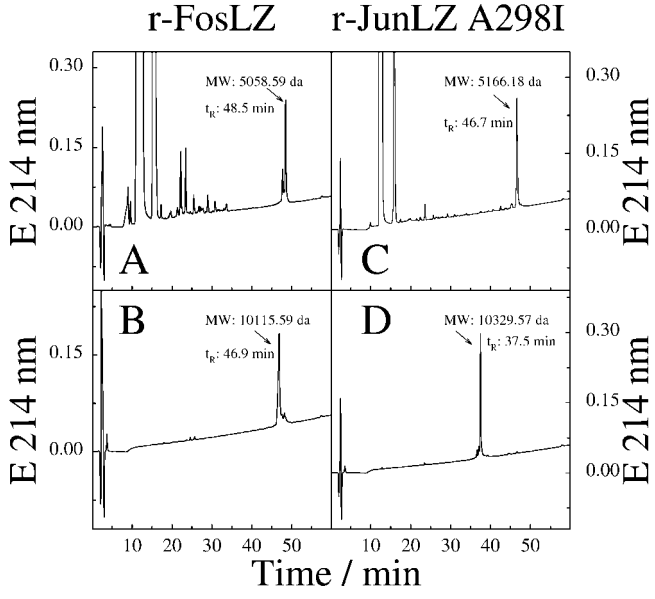

FIG. 1. **Assessment of monomer/dimer status of the r-FosLZ and r-JunLZ A298I polypeptides following elution by RP-HPLC and subsequent ESI-MS analysis after incubation for 1 h in different buffers.** *A* and *C,* in 0.2 M DTT, 0.1 M Tris-HCl, pH 8.3; *B* and *D,* in 1 mM EDTA, 0.1 M Tris-HCl, pH 8.3, respectively. No change in the elution position or molecular mass occurred when the r-FosLZ and r-JunLZ A298I polypeptides were incubated for 1 h in 30% (v/v) ACN, H_2O, 0.09% trifluoroacetic acid prior to the RP-HPLC-ESI-MS analysis.

with the unfolding of polypeptides/proteins, ΔG^0_{unfold}, in bulk solution, or at solid/liquid interfaces also often show similar parabolic dependences on temperature. The temperature at which ΔG^0_{unfold} reaches a maximum is, however, not the temperature at which the maximum stability of the polypeptide/protein is achieved. According to Klotz (41), such dome-shaped temperature effects can be interpreted in terms of parallel changes in water structure that occur during the unfolding and/or ligand binding behavior of polypeptides/proteins in such two-phase systems (42). Analogous dependences have been observed for the transfer equilibrium of many non-polar mole-

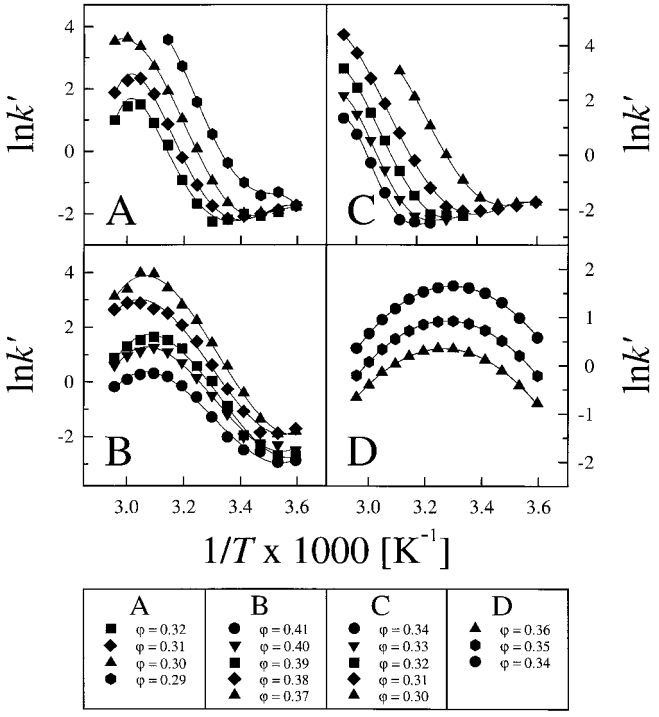

FIG. 2. **Van't Hoff plots of ln*k′* *versus* 1/*T* for the polypeptides r-JunLZ dimer (*A*), r-FosLZ dimer (*B*), r-unA298ILZ dimer (*C*), and r-JunA298ILZ monomer (*D*) at different φ values.**

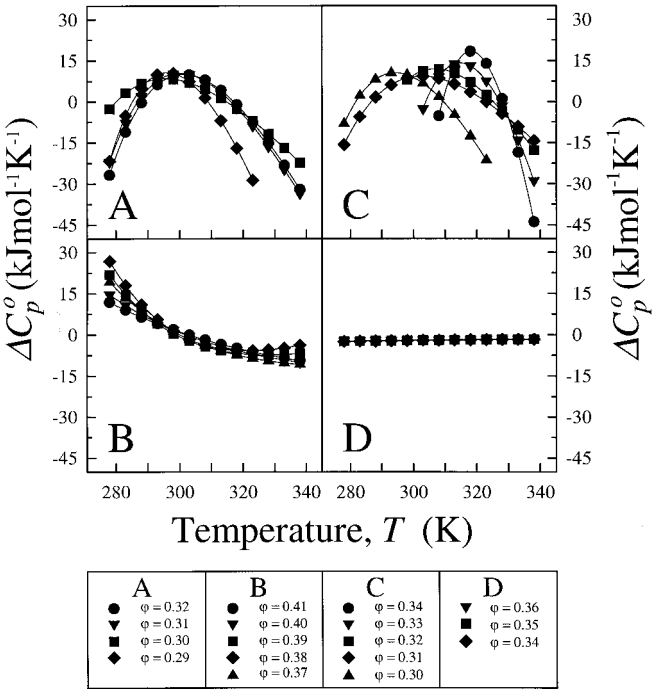

FIG. 3. **Effect of change in solvent composition on the stability of the r-Jun and r-Fos polypeptides as assessed from the plots of the change in heat capacity ΔC_p^0 for the polypeptides r-JunLZ dimer (*A*), r-FosLZ dimer (*B*), r-JunA298ILZ dimer (*C*), and r-JunA298ILZ monomer (*D*) at different temperature and φ values.**

cules to water from a less polar solvent environment as well as for more polar molecules, such as peptides, from water to non-polar environments. Such behavior can be rationalized in terms of the hydrophobic effect, with the change in the entropy of the system predominantly providing the driving force for the interaction between the polypeptide and immobilized *n*-alkyl ligand(s) over an appropriate temperature range. The dome-shaped or sigmoidal temperature dependences of these leucine zipper polypeptides is thus a further example of a widely distributed phenomenon in biology, particularly associated with the entropy-driven docking of ligands to proteins and attendant conformational changes that involve displacement of water molecules from binding sites that previously were filled with a network of structured water molecules. The differences evident in the interactive behavior of the r-Fos/r-Jun polypeptides as *T* was increased can thus be attributed to changes in the extent of solvation of surface-exposed amino acid residues of the polypeptide(s) that occur in a manner analogous to that found with G-protein-coupled receptors and ligand-gated ion channels (43, 44).

The Change in Heat Capacity Associated with the Polypeptide Ligand Interaction—The changes in heat capacity, ΔC_p^0 with respect to the *T* for these Fos/Jun leucine zipper polypeptides in association with the *n*-octyl ligands is shown in Fig. 3. The plots for the r-Jun298ILZ monomer (Fig. 3*D*) follow a similarly shaped dependence to those found with polypeptides or globular proteins of high α-helical content, *e.g.* human immunodeficiency virus, type I, gp120 CD4-binding site analogues or cytochrome *c* (27),[4] on binding to *n*-alkyl ligands under similar conditions. Collectively, these studies show that for α-helical polypeptides or globular proteins that do not significantly change their conformation in the presence of *n*-alkyl-ligands of different chain lengths due to temperature changes, only relatively small changes in ΔC_p^0 arise. For r-Jun298ILZ monomer ΔC_p^0 values were in all cases negative, indicating that the hydrophobic effect dominates the interaction of this polypeptide with the *n*-octyl ligands (46). At higher *T* values, these values progressively became more positive. Typical of these observations, the incremental change in heat capacity, $\Delta\Delta C_p^0$, for the r-Jun298ILZ monomer over the studied temperature range (ΔT = 60 K) in a solvent system of φ = 0.34 was $\Delta\Delta C_{p(\Delta T=60\text{K})}^0$ = 17.4 Jmol^{-1} K^{-1}/residue. The magnitude of $\Delta\Delta C_p^0$ for the r-Jun298ILZ monomer is comparable with $\Delta\Delta C_p^0$ values obtained for other monomeric α-helical polypeptides, *e.g.* the leucine zipper polypeptide DP-107, derived from the Asn^{558}–Gln^{595} sequence region of the envelope glycoprotein gp160 of HIV-1$_{LA1}$, where a value of $\Delta\Delta C_{p(\Delta T=60\text{K})}^0$ = 18.5 Jmol^{-1} K^{-1}/residue has been determined[5] for a solvent system with an acetonitrile volume fraction of φ = 0.41. In contrast, parabolic plots were observed for the dependence of ΔC_p^0 on *T* for the r-JunLZ and r-JunLA298ILZ dimers at different φ values over the studied ranges of $0.29 \leq \varphi \leq 0.32$ and $0.30 \leq \varphi \leq 0.34$, respectively (Fig. 3, *A* and *C*). Compared with the r-FosLZ dimer or the r-Jun298ILZ monomer, these Jun/Jun dimers exhibited substantially different ΔC_p^0 dependences on *T* (Fig. 3, *B* and *D*). Because the r-Jun298ILZ monomeric polypeptide adopts an amphipathic helical structure at room temperature, its unfolding at higher temperatures will decrease the hydrophobic contact area of the polypeptide in association with the non-polar ligands. As evident from Fig. 4*D*, the interaction between the r-Jun298ILZ monomer and the immobilized *n*-octyl ligands is associated with negative ΔH_a^0 values above *T* ≈306 K, *i.e.* the polypeptide-ligand interaction becomes increasingly exothermic at $T > 306$ K and an enthalpy-driven process due to the progressive resolvation of the polypeptide and decreased hydrophobic interaction with the non-polar ligands. Near *T* ≈306 K, ln*k′* for the r-Jun298ILZ monomer has a maximum value in the van't Hoff plots (Fig. 2*D*), consistent

[4] R. I. Boysen, A. J. O. Jong, and M. T. W. Hearn, manuscript in preparation.

[5] A. J. O. Jong, R. I. Boysen, and M. T. W. Hearn, manuscript in preparation.

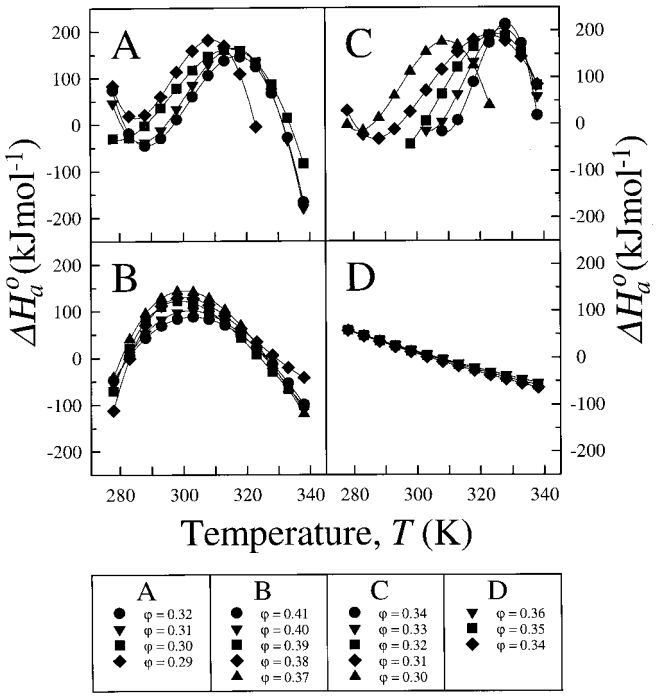

FIG. 4. **Plots of the change in enthalpy ΔH_a^0 for the interaction of the polypeptides r-JunLZ dimer (*A*), r-FosLZ dimer (*B*), r-JunA298ILZ dimer (*C*), and r-JunA298ILZ monomer (*D*) at different temperature and φ values.**

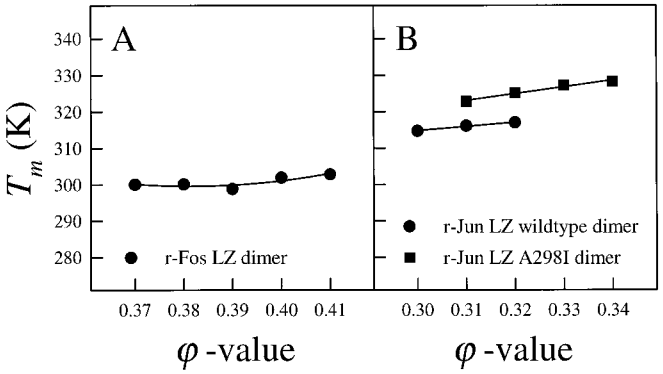

FIG. 5. **Effect of change in solvent composition on the stability of the leucine zipper polypeptides r-FosLZ dimer (*A*) and r-JunLZ dimer (*B*) and r-JunA298I LZ dimer as assessed from the plots of the melting temperature, T_m, *versus* the volume fraction, φ, of acetonitrile in the water/organic solvent mixture.**

with the r-Jun298ILZ monomer having a compensation temperature for unfolding near this temperature.

The heat capacity plots of the r-JunLZ and r-Jun298ILZ dimers are depicted in Fig. 3, *A* and *C*. For the r-JunLZ dimer (Fig. 3*A*), a decrease in the ΔC_p^0 associated with the polypeptide-ligand interaction occurs from $T \approx 296$–301 K, with ΔC_p^0 progressively becoming more negative at higher T values. The trends in ΔC_p^0 values corresponding to $\ln k'$ values >0 (*i.e.* when ΔG_a^0 values are negative) are of particular interest, because under these conditions polypeptide-ligand interactions prevail. The increasingly negative ΔC_p^0 values at $T \geq 300$ K for the r-JunLZ dimer indicate enhanced burial of the hydrophobic surface of this polypeptide. For the r-JunLZ dimer, a similar temperature optimum existed at all φ values (Fig. 3*A*). A progressive shift in the maximum occurred in the ΔC_p^0 *versus* T plots for r-Jun298ILZ dimer compared with r-JunLZ dimer at the same φ value as T was increased, with more profound changes in the position of the temperature maxima of the r-Jun298ILZ dimer in terms of the dependence on solvent composition (Fig. 3, *A* and *C*). These observations follow the thermal stabilization pattern expected for the Ala → Ile substitution and are in accord with previous CD measurements of the thermal melt profiles. Moreover, these studies are consistent with the recent observations of Dürr and Jelesarov (48) related to the energetic consequences of a cavity introduced by Leu/Ala substitutions at the tightly packed interface of the engineered dimeric leucine zipper A_2. The $\Delta\Delta C_{p,T}^0$ values of both the r-JunLZ and the r-Jun298ILZ dimers were consequently large compared with the corresponding value for the monomer (*e.g.* for the r-Jun298ILZ dimer at $\varphi = 0.31$, $\Delta\Delta C_{p(\Delta T=35\text{K})}^0 \approx 256.6$ Jmol^{-1} K^{-1}/residue in comparison to $\Delta\Delta C_{p(\Delta T=60\text{K})}^0 \approx 17.4$ Jmol^{-1} K^{-1}/residue for the r-Jun298ILZ monomer at $\varphi = 0.34$). Because the $\Delta\Delta C_{p,T}^0$ values of these leucine zipper monomer and dimer polypeptides differ by a factor of at least 15, it can be concluded that their surface areas in contact with the immobilized *n*-octyl ligands are also significantly different.

As evident from the van't Hoff plots, the leucine zipper polypeptide dimers show (Fig. 2) very small k' values (compared with the monomers) under the chosen experimental conditions at low temperatures, a finding that is consistent with the conclusion that the more compact coiled-coil molecules have buried most of their hydrophobic residues at the dimer interface. The *a* and *d* layers of the dimer interface have been shown to exhibit "knobs-into-holes" packing according to the Crick model (49), thus minimizing the exposure of the *d*-positioned Leu residues, as well as the interfacial valine residues. As T was increased, the disulfide-bridged dimers progressively unwind, exposing their hydrophobic core that can now interact with the non-polar ligands until maximum binding is reached, resulting in the observed sigmoidal van't Hoff plots for all Fos and Jun dimers. The r-FosLZ dimer achieved its maximum binding at $T \approx 324$–328 K, whereas the r-JunLZ dimer reached its maximum at $T \approx 331$–335 K. Curvilinear plots were also observed for the Ala replacement mutant r-JunA298ILZ, although the dependence of $\ln k'$ on T for this polypeptide did not reach a plateau over the investigated temperature range.

Based on Equation 14, the calculated transition midpoint melting temperatures, T_m values, of the r-FosLZ leucine zipper homodimer in different buffers fell within the range of $T \approx 299$–303 K (Fig. 5*A*), and for the r-JunA298ILZ homodimer and r-JunLZ homodimer within the range of $T \approx 323$–328 and ≈315–317 K, respectively (Fig. 5*B*). The T_m values of both Jun homodimers showed linear dependences on the φ values. The T_m value of the (Ala^{298} → Ile) r-JunA298I LZ homodimer mutant at, for example, $\varphi = 0.32$ was 9 K higher than the r-JunLZ homodimer, indicating that an enhanced thermostability has occurred due to a better packing of the hydrophobic interface within the (Ala^{298} → Ile)-substituted mutant homodimer. The derived T_m values are thus measures of the relative thermal stability of the dimeric polypeptides, reflecting the molecular composition of the dimer interface. These findings are in agreement with results obtained from CD spectroscopy, where r-JunLZ homodimer showed a melting temperature of 309 K and the r-JunA298ILZ homodimer a melting temperature of 337 K in 4 M urea (19, 20). The substantial differences between the plots of ΔC_p^0 *versus* T for the r-JunLZ and r-FosLZ homodimers, and their corresponding dependences of ΔH_a^0 and ΔS_a^0 on T, indicate moreover that the overall packing of the r-FosLZ homodimer is not perfect (50). Although Lys^{176} and Lys^{90} in the *a*-position of the coiled-coil of r-FosLZ homodimer appear to violate the hydrophobic nature the heptad repeat core, it is anticipated that the ϵ-amino groups of the lysine residues present as positive charged entities in buffers of low pH will be exposed to the solvent, whereas the methylene groups of the Lys side chains can participate in the hydrophobic

contact. In investigations (9) into the melting points in free solution of leucine zipper molecules differing only by a 3-amino acid shorter linker sequence, namely r-FosLZ homodimer, r-JunLZ homodimer, and r-Fos-r-JunLZ heterodimer, the T_m values were determined by CD spectroscopy in the absence of GdnHCl and found to be 332, 342, and 344 K, respectively. These studies confirmed that the stability of the r-FosLZ homodimer was pH-dependent with maximum stability at low pH, whereas the r-Fos-r-JunLZ heterodimer had the highest thermal stability. Because the r-Jun dimers used in the present investigation are disulfide-bridged, the observed effects are not expected to be polypeptide concentration-dependent assuming that no tetrameric species exists and the helix orientation within each dimer is parallel. This has been shown (9) to be the case for r-FosLZ homodimer and the r-JunLZ homodimer over the concentration range from 0.7 to 15 μM.

The most distinctive thermodynamic feature associated with the burial of the hydrophobic surfaces of a polypeptide or protein upon interaction with a non-polar ligand environment is a large and negative ΔC_p^0 value (51), whereas the burial of polar surface regions with a non-polar environment has a positive ΔC_p^0 value of small magnitude (52). It is widely accepted that ΔC_p^0 is proportional to the accessible surface area (53) of a polypeptide or protein that is undergoing a partitioning or adsorption event into either a non-polar environment (where the energetics of association with the immobilized ligands are largely related to entropy-driven processes due to the hydrophobic effect) or a polar environment (where the energetics of association are mediated via more significant hydrogen bonding or electrostatic contributions). The accessible surface area values for the super-helical twisted r-JunLZ homodimer (and its monomers) were calculated from solution NMR data and found to be 7241.7 Å^2 and for the monomers were 4366.7 and 4369.3 Å^2, respectively. The buried surface area, which corresponds to the monomer-monomer interface area, $\Delta A_{\text{interface}}$ was ~1494 Å^2 for the r-JunLZ dimer. Because disassembly of the super-helical twisted disulfide bridged dimers and unwinding of the α-helices will occur as T increases, changes in ΔC_p^0 as determined in the present study cannot directly be correlated with variations in the $\Delta A_{\text{interface}}$ values.

Changes in Entropy and Enthalpy and Their Compensating Effects—As apparent from Fig. 4*D* for the monomeric r-JunA298ILZ ΔH_a^0 follows a quasilinear dependence on T, whereas nonlinear dependences are apparent for all dimeric polypeptides, namely r-JunLZ, r-FosLZ, and r-JunA298ILZ (Fig. 4, *A–C*). Similar trends were evident for ΔS_a^0 for these leucine zipper polypeptides (data not shown.) When ΔH_a^0 was plotted against ΔS_a^0, linear entropy-enthalpy compensation trends are apparent for both the monomeric and the dimeric forms of these leucine zipper polypeptides (Fig. 6). From Figs. 4 and 7 it is obvious that the magnitudes of the ΔH_a^0 values are quite large compared with the corresponding ΔG_a^0 values for the polypeptide-ligand interaction. Entropy-enthalpy compensation (EEC) represents an extrathermodynamic relationship, whereby a reciprocal dependence exists between ΔH_a^0 and ΔS_a^0 when the magnitude of ΔH_a^0 are $\gg \Delta G_a^0$. Although the participation of entropy-enthalpy compensation is not a universally necessary thermodynamic criterion, in view of its widespread occurrence associated with protein folding behavior or protein-ligand interactions in bulk solution (54–57), the occurrence of EEC can be considered to reflect a particular pattern of molecular processes (58) and consequently provides an empirical attribute of the experimental thermodynamic data. In a strict thermodynamic context, the origin of enthalpy-entropy compensation involves (59) molecular reorganization of the associated structured water during protein folding/unfolding or protein-ligand interaction. The occurrence of similar EEC effects

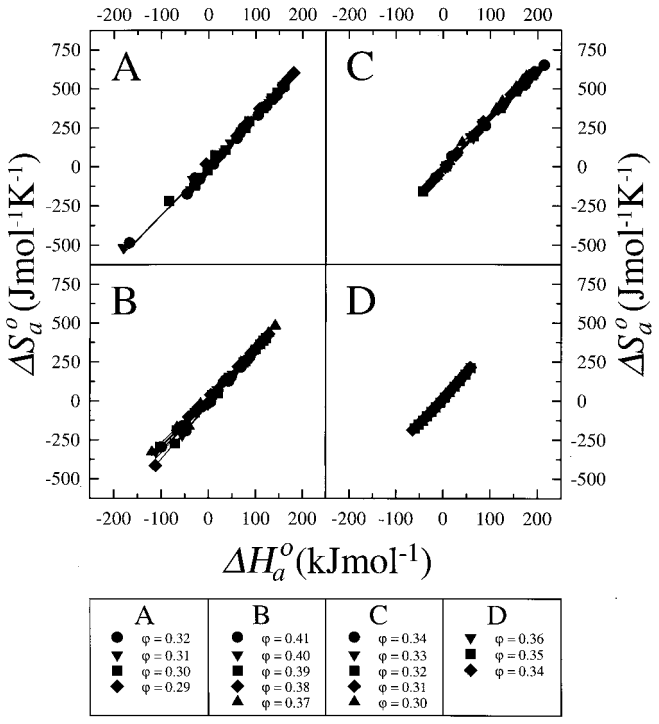

FIG. 6. **Determination of the extent of enthalpy-entropy compensation from the plots of the change in enthalpy ΔH_a^0 *versus* the change in entropy ΔS_a^0 for the polypeptides r-JunLZ dimer (*A*), r-FosLZ dimer (*B*), r-JunA298ILZ dimer (*C*), and r-JunA298ILZ monomer (*D*) at different φ values.**

for the r-FosLZ, wild type r-JunLZ, and r-JunA298ILZ polypeptides confirms that essentially the same pattern of molecular interactions comprising multiple, weak, intermolecular forces (55, 60) governs the polypeptide-non-polar ligand interactions with coiled-coil destabilization preceding α-helix unfolding as a hierarchical two-state or more complex stepwise mechanism as the temperature is increased. However, the entropy-enthalpy compensation plots of these leucine zipper polypeptides provide only partial insight into the molecular origins of the free energy changes and corresponding compensation temperatures, T_{Comp} values, which are the slope of the ΔH_a^0 *versus* ΔS_a^0 plots and characteristic parameters of the system. Thus, when the T_{Comp} values of a polypeptide in the presence of solvents of different composition are very similar, the interactions of the polypeptide with the *n*-alkyl ligands at different temperatures can be considered to be at iso-equilibrium and driven through the hydrophobic effect. To assess quantitatively the contribution of the enthalpy change, ΔH_a^0, and the corresponding entropy change, ΔS_a^0, to the Gibbs free energy of the polypeptide-non-polar ligand complex, the values of ΔG_a^0 were derived from Equation 4, and the values of ΔH_a^0 and $T\Delta S_a^0$ were plotted against T. As exemplified from the results for the r-JunA298ILZ monomer at φ = 0.34 (Fig. 8), the enthalpy (ΔH_a^0) and entropy ($T\Delta S_a^0$) functions are non-linear and intersect each other at two points just outside the measured temperature range corresponding to the cold and hot compensation points, T_{Cold} = 271.2 K and T_{Hot} = 342.1 K. Below T_{Cold} or above T_{Hot} ΔG_a^0 becomes positive, indicative of an unfavorable protein-ligand interaction.

Fig. 8 can be divided into three regions, A, B, and C, defined by the corresponding compensation temperatures T_H (where ΔH_a^0 = 0) and T_S (where ΔS_a^0 = 0). In region A, $\Delta H_a^0 > 0$ (destabilizing with regard to the protein-ligand interaction) and $\Delta S_a^0 > 0$ (stabilizing with regard to the interaction). In region B, $\Delta H_a^0 < 0$ and $\Delta S_a^0 > 0$ (both stabilizing with regard to

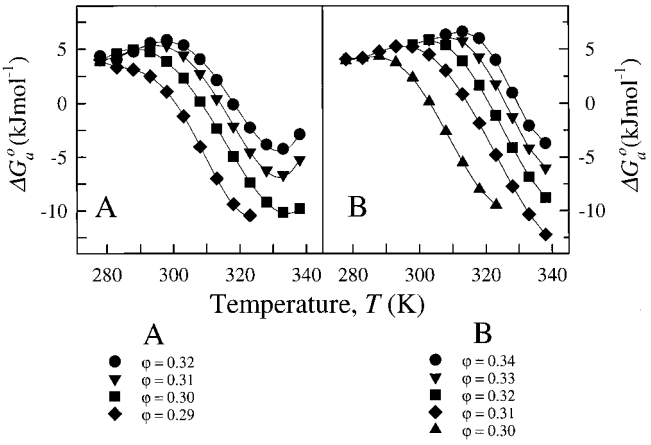

FIG. 7. **Plots of Gibbs free energy ΔG_a^0 *versus* T for the polypeptides r-JunLZ dimer (*A*) and r-JunA298ILZ dimer (*B*).**

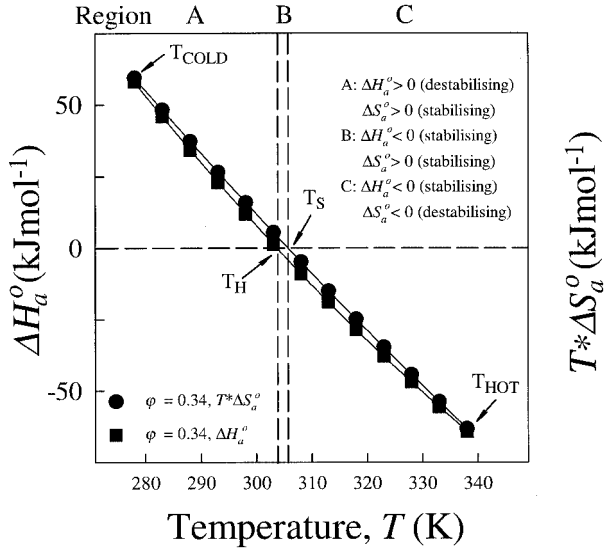

FIG. 8. **Determination of the Gibbs free energy balance from the plots of ΔH_a^0 and ΔTS_a^0 *versus* T for r-JunA298I LZ monomer at a φ value of 0.34 using a water/acetonitrile solvent mixture.**

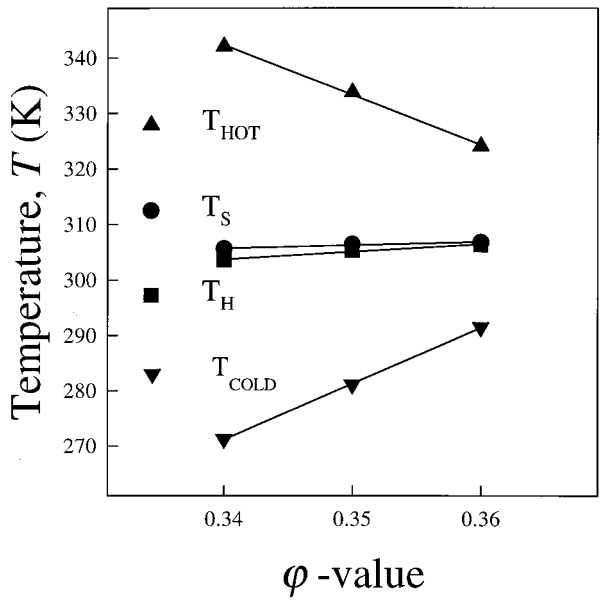

FIG. 9. **Plots of compensation temperatures T_S, T_H, T_{Cold}, and T_{Hot} *versus* the volume fraction, φ, of acetonitrile in the bulk solvent for the r-JunA298I LZ monomer.**

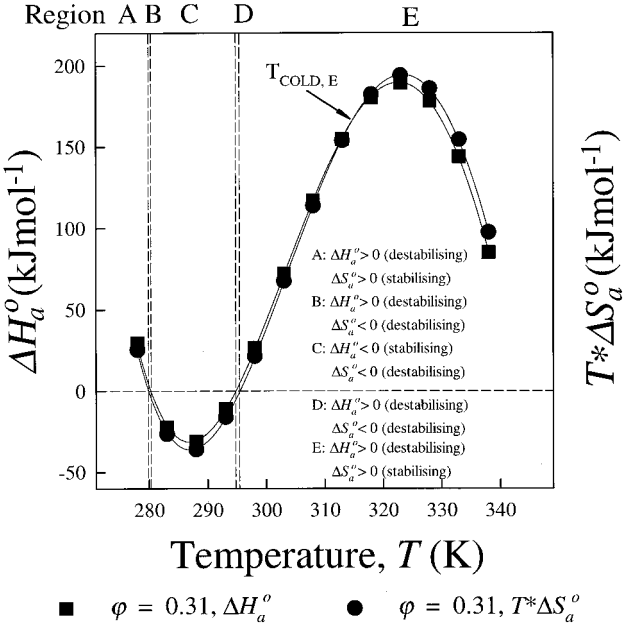

FIG. 10. **Plot of Gibbs free energy balance, calculated from ΔH_a^0 and ΔTS_a^0, *versus* T for r-JunA298I LZ dimer at a φ value of 0.31 using a water/acetonitrile solvent mixture.**

the interaction). In region C, $\Delta H_a^0 < 0$ (stabilizing with regard to the interaction) and $\Delta S_a^0 < 0$ (destabilizing with regard to the interaction). Below the compensation temperature, *e.g.* $T_{H(\varphi=0.34)} \approx 303.6$ K, the interaction is entropically driven, whereas above the compensation temperature, *e.g.* $T_{S(\varphi=0.34)} \approx 305.6$ K, the interaction progressively becomes more enthalpically driven, with greater solvation of the amino acid side chains.

Region B represents the temperature range were the protein-non-polar ligand interaction reaches its maximal (enthalpy and entropy both drive a favorable interaction) and corresponds to the maximum in the van't Hoff plot (*cf.* Fig. 2*D*). As shown in Fig. 9, for r-JunA298ILZ monomer the compensation temperatures, T_S and T_H, show a nearly linear temperature dependence on φ. This dependence is consistent with water re-organization as the physical origin of the enthalpy-entropy compensation effect with these leucine zipper polypeptides (55, 56), with entropy-enthalpy compensation, strictly speaking, limited to the temperature range between T_{Cold} and T_{Hot}. Above the T_{Hot} point, the dominant term of the Gibbs energy balance is the entropic term. Here the gain of conformational freedom, caused by the rising temperature, is not compensated by the change in enthalpy. Below the T_{Cold} point, the dominant enthalpically driven interaction of the leucine zipper polypeptides with the solvent will tend to destabilize the polypeptide-non-polar ligand association, with the polypeptides, from an energetic point of view, preferring to be fully solvated.

The Gibbs free energy balance plot for the r-JunA298ILZ dimer and the results are shown in Fig. 10. In this case, five regions can be identified from the compensation temperatures T_H ($\Delta H_a^0 = 0$) and T_S ($\Delta S_a^0 = 0$), depending on the dominance of the enthalpy or entropy term. In particular, in region E, it can be seen that above the cold compensation point $T_{Cold,E}$ the Gibbs free energy ΔG_a^0 becomes negative, *i.e.* $\Delta H_a^0 < \Delta TS_a^0$, and defines a conditional range were polypeptide-ligand interactions are favored at higher temperatures despite the fact that the enthalphic contribution is destabilizing, *i.e.* $\Delta H_a^0 > 0$. Collectively, the EEC plots (Fig. 6) and the Gibbs free energy balance plots (Fig. 8 and 10) provide the thermodynamic signatures of these leucine zipper polypeptides in these systems,

whereby T_{Cold} and T_{Hot} define the temperature range over which the EEC occurs, and T_H and T_S define the temperature range at which the change in enthalpy or the change in entropy provide the driving force to preferentially stabilize the leucine zipper polypeptide-ligand interaction.

As apparent from the above results with the monomeric and dimeric polypeptides related to the leucine zipper transcription factors Fos and Jun, the current investigation exemplifies the use of a newly developed technique to monitor the conformational transitions and stability of native and mutant polypeptides/proteins. In the specific case investigated, the transition from a coiled-coil polypeptide to an uncoiled state could be qualitatively as well as quantitatively evaluated in terms of the respective thermodynamic signature of the polypeptide-ligand interaction. These procedures enable the direct assessment of the thermal stability of closely related polypeptides/proteins in the presence of hydrophobic or other types of ligands. In particular, this investigation demonstrates the advantages of this new thermometric approach in the evaluation of the complex influences of mutational and solvational effects on protein/polypeptide stability. A further advantage relates to the ability to monitor the complex thermodynamics of protein stability at temperatures other than at the midpoint unfolding temperature, T_m, over a wide range of experimental conditions. As evident from the experimental findings described above, the results on the relative thermal stability of the r-JunLZ homodimer and the r-JunA298ILZ homodimer are in good agreement with data obtained from melting experiments in free solution monitored by CD spectroscopy and correlate with the buried surface area during coiled-coil formation. In contrast to CD studies, these thermometric procedures readily permit immobilized ligand-polypeptide interactions to be investigated and the corresponding thermodynamic and extrathermodynamic parameters evaluated for a very wide variety of temperature and solvent conditions. Moreover, data acquisition can be largely automated, permitting a wide variety of experimental measurements to be acquired rapidly. It is anticipated that this approach can be utilized for the investigation of polypeptide complexes where domain-domain association follows similar hierarchical principles. Our ongoing investigations will focus on the correlation of thermodynamic values derived from the procedure described herein for globular proteins and polypeptides with stabilized secondary structures with the corresponding values obtained from microcalorimetric measurements. Results of these investigations have been reported elsewhere (61).

REFERENCES

1. Bohmann, D., Bos, T. J., Admon, A., Nishimura, T., Vogt, P. K., and Tjian, R. (1987) *Science* **238,** 1386–1392
2. Hattori, K., Angel, P., Le Beau, M. M., and Karin, M. (1988) *Proc. Natl. Acad. Sci. U. S. A.* **85,** 9148–9152
3. McLachlan, A. D., and Stewart, M.(1975) *J. Mol. Biol.* **98,** 293–304
4. Landschulz, W. H., Johnson, P. F., and McKnight, S. L. (1988) *Science* **240,** 1759–1764
5. Ramirez-Carrozzi, V. R., and Kerppola, T. K. (2001) *J. Biol. Chem.* **276,** 21797–21808
6. Ramirez-Carrozzi, V. R., and Kerppola, T. K. (2001) *J. Mol. Biol.* **305,** 411–427
7. Junius, F. K., Weiss, A. S., and King, G. F. (1993) *Eur. J. Biochem.* **214,** 415–424
8. Junius, F. K., O'Donoghue, S. I., Nilges, M., Weiss, A. S., and King, G. F. (1996) *J. Biol. Chem.* **271,** 13663–13667
9. O'Shea, E. K., Rutkowski, R., Stafford, W. F. D., and Kim, P. S. (1989) *Science* **245,** 646–648
10. Glover, J. N. M., and Harrison, S. C. (1995) *Nature* **373,** 257–261
11. Harbury, P. B., Zhang, T., Kim, P. S., and Alber, T. (1993) *Science* **262,** 1401–1407
12. Yu, Y. H., Monera, O. D., Hodges, R. S., and Privalov, P. L. (1996) *J. Biophys. Chem.* **59,** 299–314
13. Kohn, W. D., Kay, C. M., and Hodges, R. S. (1997) *J. Mol. Biol.* **267,** 1039–1052
14. Pace, C. N., Laurents, D. V., and Thomson, J. A. (1990) *Biochemistry* **29,** 2564–2572
15. O'Shea, E. K., Rutkowski, R., and Kim, P. S. (1992) *Cell* **68,** 699–708
16. Kovrigin, E. L., and Potekhin, S. A. (2000) *Biophys. Chem.* **83,** 45–59
17. Purcell, A. W., Aguilar, M. I., and Hearn, M. T. W. (1999) *Anal. Chem.* **71,** 2440–2451
18. Monera, O. D., Zhou, N. E., Kay, C. M., and Hodges, R. S. (1993) *J. Biol. Chem.* **268,** 19218–19227
19. Bains, N. P. S., Wilce, J. A., Heuer, K. H., Tunstall, M., Mackay, J. P., Bennet, M. R., Weiss, A. S., and King, G. F. (1997) *Lett. Pept. Sci.* **4,** 67–77
20. Bains, N. P. S., Wilce, J. A., Mackay, J. P., and King, G. F. (1999) *Lett. Pept. Sci.* **6,** 381–390
21. Wendt, H., Berger, C., Baici, A., Thomas, R. M., and Bosshard, H. R. (1995) *Biochemistry* **34,** 4097–4107
22. Kondejewski, L. H., Jelokhani-Niaraki, M., Farmer, S. W., Lix, B., Kay, C. M., Sykes, B. D., Hancock, R. E. W., and Hodges, R. S. (1999) *J. Biol. Chem.* **274,** 13181–13192
23. Hearn, M. T. W. (2001) in *Synthesis of Peptides and Peptidomimetics* (Goodman, M., Felix, A., Moroder, L., and Tonioloand, C., eds) Houben-Weyl-Thieme Publishers, Stuttgart, in press
24. Beyermann, M., Fechner, K., Furkert, J., Krause, E., and Bienert, M. (1996) *J. Med. Chem.* **39,** 3324–3330
25. Hearn, M. T. W. (2000) in *Handbook of Bioseparation* (Ahuja, S., ed) pp. 72–235, Academic Press, San Diego
26. Hearn, M. T. W., and Zhao, G. L. (1999) *Anal. Chem.* **71,** 4874–4885
27. Boysen, R. I., Wang, Y., Keah, H. H., and Hearn, M. T. W. (1999) *Biophys. Chem.* **77,** 79–97
28. Eisenhaber, F., and Argos, P. (1993) *J. Comput. Chem.* **14,** 1272–1280
29. Eisenhaber, F., Lijnzaad, P., Argos, P., Sander, C., and Scharf, M. (1995) *J. Comput. Chem.* **16,** 273–284
30. Berman, H. M. (1999) *Curr. Opin. Biotechnol.* **10,** 76–80
31. Sussman, J. L., Lin, D. W., Jiang, J. S., Manning, N. O., Prilusky, J., Ritter, O., and Abola, E. E. (1998) *Acta Crystallogr. Sect. D Biol. Crystallogr.* **54,** 1078–1084
32. Boysen, R. I., and Hearn, M. T. W. (2001) in *Current Protocols in Molecular Biology* (Smith, J. A., ed) John Wiley & Sons, Inc., New York, 1–32
33. Hearn, M. T. W., Boysen, R. I., Wang, Y., and Muraledaram, S. (1999) in *Peptide Science: Present and Future* (Shimonishi, Y., ed) pp. 240–244, Kluwer Academic Publishers Group, Dordrecht, Netherlands
34. Purcell, A. W., Zhao, G. L., Aguilar, M. I., and Hearn, M. T. W. (1999) *J. Chromatogr.* **852,** 43–57
35. Melander, W. R., Corradini, D., and Horvath, C. (1984) *J. Chromatogr.* **317,** 67–85
36. Hearn, M. T. W. (2001) in *Theory and Practice of Biochromatography* (Vijayalakshmi, M. A., ed) pp. 72–141, Harwood Academic Publishers, Switzerland
37. Vailaya, A., and Horvath, C. (1996) *Ind. Eng. Chem. Res.* **35,** 2964–2981
38. Haidacher, D., Vailaya, A., and Horvath, C. (1996) *Proc. Natl. Acad. Sci. U. S. A.* **93,** 2290–2295
39. Chen, B. L., Baase, W. A., Nicholson, H., and Schellman, J. A. (1992) *Biochemistry* **31,** 1464–1476
40. Ha, J. H., Spolar, R. S., and Record, M. T. (1989) *J. Mol. Biol.* **209,** 801–816
41. Klotz, I. M. (1999) *J. Phys. Chem.* **103,** 5910–5916
42. Silverstein, K. A. T., Haymet, A. D. J., and Dill, K. A. (1998) *J. Am. Chem. Soc.* **120,** 3166–3175
43. Weiland, G. A., Minneman, K. P., and Molinoff, P. B. (1979) *Nature* **281,** 114–117
44. Borea, P. A., Varani, K., Guerra, L., Gilli, P., and Gilli, G. (1992) *Mol. Neuropharmacology* **2,** 273–281
45. Deleted in proof
46. Murphy, K. P. (1999) *Med. Res. Rev.* **19,** 333–339
47. Deleted in proof
48. Durr, E., and Jelesarov, I. (2000) *Biochemistry* **39,** 4472–4482
49. Crick, F. H. C. (1953) *Acta Crystallogr.* **6,** 689–697
50. Stites, W. E. (1997) *Chem. Rev.* **97,** 1233–1250
51. Ross, P. D., and Rekharsky, M. V. (1996) *Biophys. J.* **71,** 2144–2154
52. Murphy, K. P., and Gill, S. J. (1991) *J. Mol. Biol.* **222,** 699–709
53. Robertson, A. D., and Murphy, K. P. (1997) *Chem. Rev.* **97,** 1251–1267
54. Lumry, R., and Rajender, S. (1970) *Biopolymers* **9,** 1125–1227
55. Dunitz, J. D. (1995) *Chem. Biol.* **2,** 709–712
56. Mallardi, A., Giustini, M., and Palazzo, G. (1998) *J. Phys. Chem.* **102,** 9168–9173
57. Dill, K. A. (1990) *Biochemistry* **29,** 7133–7155
58. Gallicchio, E., Kubo, M. M., and Levy, R. M. (1998) *J. Am. Chem. Soc.* **120,** 4526–4527
59. Liu, L., Yang, C., and Guo, Q. X. (2000) *Biophys. Chem.* **84,** 239–251
60. Tehan, M. C., Choy, K. J., Mackay, J. P., Lyons, A. T., Basins, N. P. S., and Weiss, A. S. (2000) *J. Biol. Chem.* **275,** 37454–37461
61. Lin, F.-Y., Chen, W.-Y., and Hearn, M. T. W. (2001) *Anal. Chem.* **73,** 3875–3883

Role of Interfacial Hydrophobic Residues in the Stabilization of the Leucine Zipper Structures of the Transcription Factors c-Fos and c-Jun

Reinhard I. Boysen, Agnes J. O. Jong, Jackie A. Wilce, Glenn F. King and Milton T. W. Hearn

J. Biol. Chem. 2002, 277:23-31.
doi: 10.1074/jbc.M104556200 originally published online October 15, 2001
